Measurement of porosity as a predictor of the performance of concrete with and without Silica Fume

Claisse, P.A. , Cabrera, J.G. and Hunt, D.N.

Advances in Cement Research, 2001, **13**, No. 4, October, 165–174

Measurement of porosity as a predictor of the durability performance of concrete with and without condensed silica fume

P. A. Claisse,* J. G. Cabrera† and D. N. Hunt*

Coventry University; Leeds University

The objective of this article is to investigate the use of porosity as a predictor of the properties of concrete that control its durability. In particular concretes containing silica fume (SF) have been investigated. Four different mixes were made, two containing SF and two control mixes without SF. The mixes were tested using three different curing conditions and three different test ages. The porosity was measured with helium intrusion, mercury intrusion and by calculation from weight loss observations. A wide range of durability related properties were measured and the results correlated with the porosities. It is concluded that the porosity is an excellent predictor for the transport properties but less good for actual corrosion rates. It is also indicated that models developed for concretes without SF should be used with great caution for SF concretes.

Introduction

The porosity (i.e. the volumetric proportion of voids) of concrete has been used extensively for the prediction of the properties of concrete.[1] The objective of this article is to compare three different measurements of porosity, to show how effective they are as predictors of durability performance related properties of concrete and to show how the predictive models are affected by the use of silica fume (SF) in the concrete.

SF has been in use in concrete as a cementitious component for some years[2] and has been shown to refine the pore structure.[3] It has been shown that the relationships between different properties of SF concrete are different from those for concrete without SF (PC concrete)[4] and it is therefore important to check whether reduction in porosity in SF concretes has the same effect as it has in PC concretes.

In this article three different measurements of porosity have been used: mercury intrusion; helium intrusion; and calculations from measurements of weight loss. Mercury intrusion is the only one of these which gives data on the relative contribution of pores from different size ranges to the total porosity (e.g. refinement of the pore structure). Kumar *et al*.[5] used the value of the mean pore radius in the range 0·002–7·5 μm as a measure of the effect of SF replacement. Using 28 day curing at 60°C they found this median radius for a 10% SF paste to be less than 40% of the radius for PC paste. Other workers[6] have calculated porosities for different pore size ranges. This method is used in this article. The pores in the 1–2 μm range have been observed with an electron microscope.[7]

Experimental methods

Sample preparation

Samples were prepared to the four different mix designs given in Table 1. Mortar samples were made with the same proportions but without the coarse aggregate. Paste samples were made with the sample proportions but without the coarse or fine aggregates. After casting the samples were covered and kept at 20°C for 24 h until they were struck. They were then cured using the three different curing conditions given in Table 2.

The samples were tested at 3, 28 and 90 days. All

* School of Built Environment, Coventry University, Priory Street, Conventry, CV1 SFB, UK.
† J. G. Cabrera (deceased), formerly of Leeds University, Leeds, UK

(ACR 378) Paper received 23 January 2001; last revised 27 June 2001; accepted 9 July 2001.

Table 1. Mix designs

Mix	A	B	C	D
Cement (kg/m^3)	344	430	252	315
SF (kg/m^3)	86	0	63	0
Water/(PC + SF)	0·3	0·3	0·46	0·46
Superplasticiser (% of PC + SF)	1·4	1·4	1·9	1·9
5–20 mm aggregate/(PC + SF)	3	3	4	4
Fine aggregate/(PC + SF)	1·5	1·5	2·3	2·3

Table 2. Curing conditions

Curing condition (CC) No.	
1	20°C and 99% RH until test age
2	Treated with aluminium pigmented curing agent and kept at 20°C for 7 days and then in water at 6°C
3	In water at 6°C until test age

combinations of the four mixes, three curing conditions and three test ages were used for the tests giving a total of 36 'sample conditions' that reflect a wide range of possible conditions for site concrete when first exposed to an aggressive environment. Different types of sample were used for the different tests as described below. No study was made of the surface properties of concrete, so for all samples used to measure transport properties samples were cut from the centres of the specimens and the outer surfaces were not tested.

Sample testing

The test that were carried out are summarised in Table 3. The authors emphasise that these are not, and could not be, a completely comprehensive set of measurements of durability related properties. The work could have been continued to measure chemical attack on concrete, freeze thaw, etc. Similarly, other transport properties such as the permeability to fluids other than oxygen could be measured. The tests in Table 3 are, however, proposed as a representative sample of the available tests. Compressive strength was measured because this is the property that is most often known for concrete mixes.

Table 3. Summary of test programme

Test	Material	Ref
Porosity measurements		
Mercury intrusion	Paste	10
Helium intrusion	Paste/mortar/concrete	10
Weight loss	Paste/mortar/concrete	10
Transport property measurements		
Chloride transport	Concrete	8
Carbonation	Mortar	10
Oxygen transport	Mortar	9
Water vapour transport	Paste	9
Corrosion measurements		
Initial corrosion current	Concrete	11
28 day corrosion current	Concrete	11
Other properties		
Compressive strength	Concrete	–
Initial resistivity	Concrete	11
28 day resistivity	Concrete	11

Porosity measurements

Mercury intrusion. Cylindrical samples of paste with a diameter of 25 mm and a length of approximately 15 mm were intruded using a Micromeritics Auto-Pore 9200 intrusion machine. The machine has a maximum operating pressure of 414 MPa. The diameter of the pores was obtained using equation (1)

$$D = \frac{-4\gamma \cos \phi}{p} \quad (1)$$

where: D is the diameter of the smallest pore that the mercury can enter; γ is the surface tension of the mercury; ϕ is the contact angle of the mercury with the pore surface; p is the pressure.

The values used for the contact angle and the surface tension of the mercury were 130° and 0·484 N/m which give a minimum pore diameter of 0·003 μm at the highest pressure.

Helium intrusion. The net volume of samples was measured by helium intrusion using a Micromeritics Autopycnometer 1320. The samples were ground to pass a 1·18 mm sieve before testing to ensure full penetration into the pore structure. The samples were weighted before testing and the specific gravity was calculated as the mass divided by the net volume.

Measurement of weight loss. For this purpose samples were cast in disposable plastic cups. This method was used because the cups were convenient and did not require mould oil which would have affected the weight. The following weights were recorded.

(*a*) Wet weight when cast.
(*b*) Weight of empty cup when sample struck (24 hours after casting).
(*c*) Wet and surface dry weights after curing.
(*d*) Dry weights after drying to constant weight in ventilated oven at 110°C.

Measurement of transport properties

Chloride transport. Chloride transport was measured by placing sodium chloride solutionin holes drilled in concrete samples. After exposure the bases of the holes were drilled and dust samples collected from different depths and analysed for chloride content. Details of the experimental procedure are given in reference.[8]

Carbonation. Mortar samples measuring 25 mm × 25 mm × 200 mm long were exposed to an atmosphere of 90% CO_2 at a pressure of 1 bar at 21°C and

70% RH. The shrinkage was measured at 18 days after exposure with a comparator using a Linear Voltage Displacement Transducer (LVDT). The recorded strain was a total arising both from the carbonation and from drying shrinkage while in the carbonation chamber.

Oxygen transport. Sections 20 mm long of 25 mm mortar cores were tested for oxygen transport under an applied pressure difference of 1 and 2 bar. Details of the procedure are in reference.[9]

Water vapour transport. Discs 4 mm thick of paste were sealed into the lids of bottles with water in them. The bottles were then placed in controlled humidity environments and their weight loss recorded. Details of the procedure are in reference.[9]

Compressive strength. This was measured on 100 mm cubes.

Corrosion measurements

Samples containing a mild steel bar were placed in salt solution and the initial corrosion rates and were obtained from linear polarisation resistance measurements. The steel was then polarised to +100 mV relative to a standard calomel electrode for 28 days and the corrosion rate was measured again. The resistance of the samples was measured by applying an alternating current to them. The values of resistance were used in the calculation of corrosion currents (IR compensation was not used) and also recorded as a property in their own right. Details of the experimental procedures are reported elsewhere.[10,11]

Data analysis

Two readings were obtained for each sample conditon for each experiment. The data were collected onto a microcomputer[12] and the average of each pair of readings was used for the analysis reported here.

Analysis

Calculation of porosity

Mercury intrusion. Fig. 1 shows a typical output from the mercury intrusion. In order to characterise the salient features of the intrusion curves for further analysis the total intruded volumes in varying pore size ranges was obtained from the data (see Table 4).

The recovery volume is the volume of mercury which came out of the samples when the pressure was released. These ranges are shown in Fig. 1 which shows the cumulative and differential intrusion volumes for two replicate samples with the size ranges marked with the vertical gridlines. For each range the porosity was calculated as a percentage of the bulk volume of the samples.

Helium intrusion. The helium intrusion experiment yielded results for specific gravity (SG, the mass divided by the net volume). The dry density (DD, the mass divided by the bulk volume) was obtained from

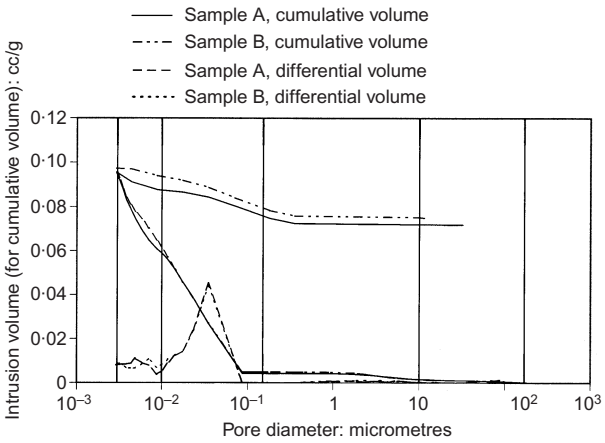

Fig. 1. Typical output from mercury intrusion. The vertical gridlines show the boundaries of the pore size ranges which were used for analysis

Table 4. Total intruded volumes for varying pore sizes

Range	Typical porosity
10–170 μm	0·5%
0·15–10 μm	0·7%
0·01–0·15 μm	16%
0·003–0·01 μm	7%
0·003–10 μm (recovery)	10%

the weight loss measurements. The porosity was then obtained from equation (2)

$$\text{Porosity} = 100\left(1 - \frac{SG}{DD}\right) \tag{2}$$

Measurement of weight loss. The porosity of the PC samples was calculated from the weight loss using the Powers model.[1] For this calculation the water and cement which combine to form hydrated cement are assumed to do so in a fixed ratio. Neville[1] uses a w/c ratio of 0·23:1 but in this work a ratio of 0·25:1 has been used because it gave a better agreement with other measurements of porosity and had been proposed previously.[13]

The weight of the samples when cast M_{wet} was obtained by subtracting the weight of the cup from the initial weight. The weight of water M_{w} in the wet sample was then calculated from the mix proportions. The dry weight M_{dry} was measured. Thus: the mass of absorbed water $M_{\text{aw}} = M_{\text{w}} - (M_{\text{wet}} - M_{\text{dry}})$; and from the assumption of the ratio of combination: the mass of hydrated cement $M_{\text{hc}} = 5 \times M_{\text{aw}}$.

The mass of each component of the hydrated sample was therefore known and the specific gravity of the sample was calculated from the equation (3).

$$\frac{M}{SG} = \Sigma\frac{M_i}{SG_i} \tag{3}$$

Where the sum is across all of the components of the

dry mix, i.e. cement, hydrated cement, aggregate (if present) and the solids in the admixtures. The specific gravity of each component was measured experimentally except for the hydrated cement for which a value of 2·15 g/cc was used.[13]

The dry density was obtained by dividing the dry mass by the volume obtained by weighing wet and dry and the porosity was then obtained from equation (2).

These equations do not work for samples containing additional components such as SF. Attempts were made to extend the model using data from Thermogravimetric analysis to determine the proportions of hydration products in the hydrated SF samples, but the porosities obtained were not consistent with other observations and are not reported in this article.

Calculation of correlations

The relationships between all of the different variables studied (data columns) was calculated as the correlation coefficient R^2. The value of this for 1% significance is 0·17 for the PC and SF samples together (a complete column of 36 values) and 0·31 for the PC or the SF samples individually (half a column – 18 values).

Results and discussion

Comparison between different measurements of paste porosity

Comparison between the different test methods. The relationship between the different measurements is shown in Figs 2 and 3. Comparisons could only be made for paste because these were the only type used for mercury intrusion. From Fig. 2 it may be seen that mercury intrusion yields a lower value than helium intrusion. This would be expected because the samples were ground for helium intrusion and the low molecular size and viscosity of the helium. The calculations of porosity were only used for the PC samples but Fig. 3 shows that these samples correlate well, with the helium results giving generally slightly lower values.

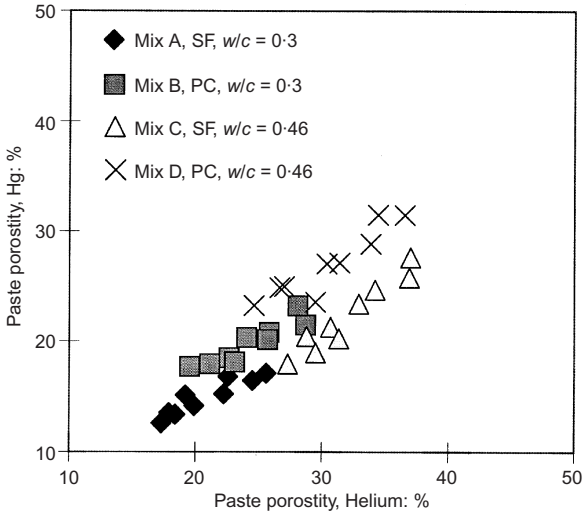

Fig. 2. Comparison of paste porosities from helium and mercury intrusion

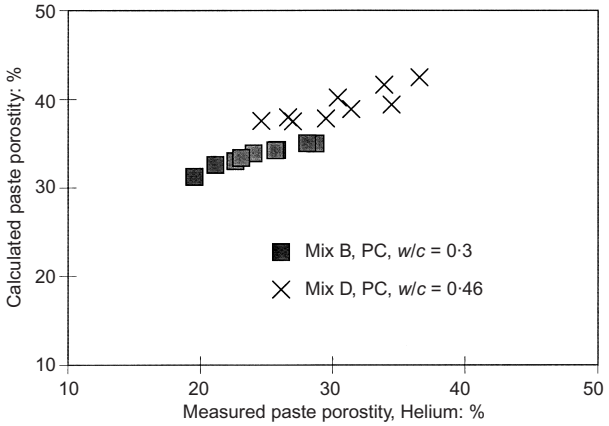

Fig. 3. Comparison of calculated paste porosity with measured porosity from helium intrusion

Porosities for different pore size range. The porosity from mercury intrusion was, as described above, sub-divided into porosities for different pore size ranges. These porosities in the different pore size ranges were correlated with the total porosities also obtained from mercury intrusion. No correlation was observed in the size range for the largest pores.

The correlation between porosities in the 0·15–10 μm range and total porosity was negative (Fig. 4). Significant values of R^2 of 0·314 for the SF samples and 0·340 for all of the samples were obtained. The negative correlation indicates that the porosity in this range, which increases with a decrease in total porosity, is unlikely to be significant in predictive models for properties which generally correlate with porosity.

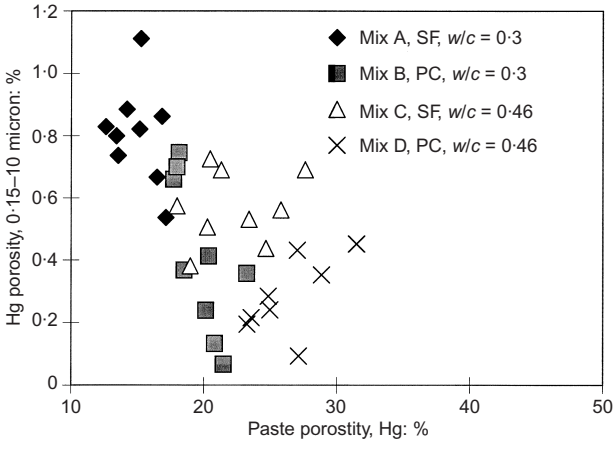

Fig. 4. Mercury intrusion porosity in the 0·15–10 μm pore size range vs. total mercury intrusion porosity

The bulk of the pores lie in the 0·01–0·15 μm range and a good correlation with the total porosity was expected. Fig. 5 shows, however, that the SF samples had significantly lower porosity in this range and the relationship with total porosity was therefore different from that for the PC mixes.

Fig. 6 for the 0·003–0·01 μm range shows the extent of the refinement of the pore structure caused by the SF, the correlations with total porosity are not significant but the effect of the SF is very clear. This refinement of the pore structure has the effect of reducing the recovery volumes for the SF samples. This may be seen in Fig. 7.

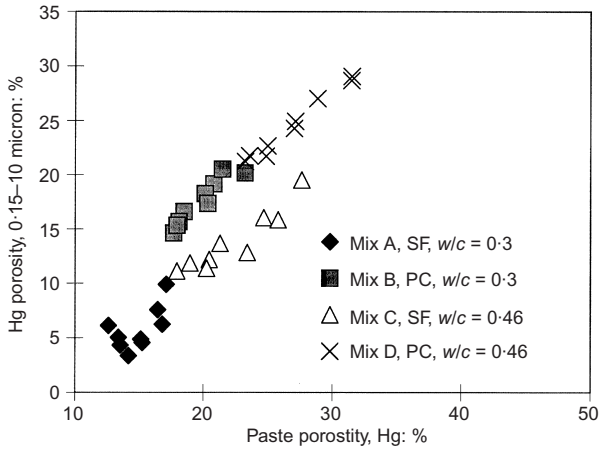

Fig. 5. Mercury intrusion porosity in the 0·01–0·15 μm pore size range vs total mercury intrusion porosity

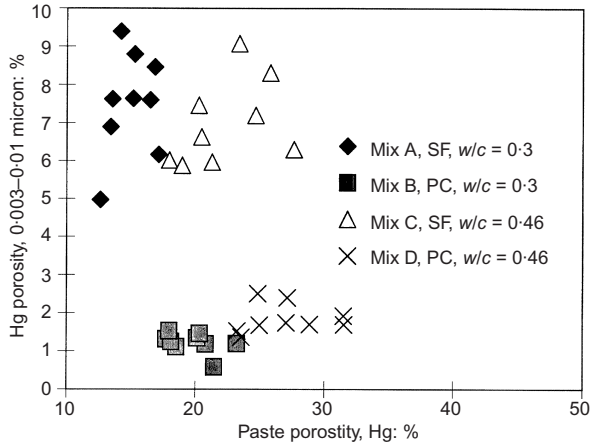

Fig. 6. Mercury intrusion porosity in the 0·003–0·01 μm pore size range vs total mercury intrusion porosity

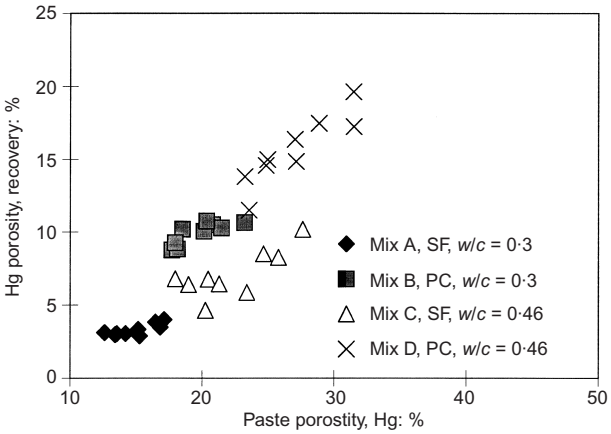

Fig. 7. Mercury intrusion recovery porosity vs. total mercury intrusion porosity

Using porosity measurements to predict durability related properties

Measurements from concrete, mortar or paste. For the Helium intrusion and the weight loss measurements tests were carried out on concrete, mortar and paste samples. When considering which of these to use as predictors for concrete properties there are two conflicting factors: measurements on concrete are theoretically the most realistic but concrete porosities are lower than those for mortar and paste so the accuracy of measurement will be lower. It is obviously possible to calculate one porosity from another with a knowledge of the proportions and porosity (if any) of the aggregate. Table 5 shows some of the correlations of porosities with properties that were measured on concrete samples.

It may be seen that the mortar results generally gave poorer correlations but neither the concrete or the paste was found to be universally better. The correlations for paste and concrete porosity for all of the measured properties are shown in Table 6.

Table 5. Comparison of correlations for paste, mortar and concrete for some properties (values of R^2)

Predictor	Type of sample	Property		
		Chloride transport	Strength	Corrosion
Measurements of porosity from helium intrusion (all samples)	Paste	0·537	0·671	0·113
	Mortar	0·376	0·295	0·393
	Concrete	0·593	0·450	0·583
Calculations of porosity from weight loss using equation (2) (PC samples only)	Paste	0·756	0·944	0·419
	Mortar	0·045	0·006	0·252
	Concrete	0·646	0·884	0·402

Table 6. Correlations—values of R^2

Property	Predictor	All	PC	SF
Chloride concentration	Paste porosity (helium)	0·537	0·730	0·661
	Concrete porosity (helium)	0·593	0·702	0·257
	Paste porosity (mercury)	0·771	0·808	0·716
	Calculated paste porosity		0·756	
	Calculated concrete porosity		0·646	
Carbonation strain microstrain	Paste porosity (helium)	0·652	0·717	0·717
	Concrete porosity (helium)	0·458	0·719	0·617
	Paste porosity (mercury)	0·625	0·788	0·698
	Calculated paste porosity		0·615	
	Calculated concrete porosity		0·700	
Log of Oxygen permeability $m^2 \times 10^{-18}$	Paste porosity (helium)	0·448	0·700	0·424
	Concrete porosity (helium)	0·645	0·743	0·428
	Paste porosity (mercury)	0·634	0·807	0·374
	Calculated paste porosity		0·741	
	Calculated concrete porosity		0·743	
Water vapour transport	Paste porosity (helium)	0·807	0·765	0·922
	Concrete porosity (helium)	0·334	0·613	0·703
	Paste porosity (mercury)	0·600	0·699	0·903
	Calculated paste porosity		0·574	
	Calculated concrete porosity		0·516	
Log of Initial corrosion current mA/m^2	Paste porosity (helium)	0·243	0·219	0·287
	Concrete porosity (helium)	0·246	0·122	0·079
	Paste porosity (mercury)	0·345	0·210	0·251
	Calculated paste porosity		0·259	
	Calculated concrete porosity		0·097	
Log of 28 day corrosion current mA/m^2	Paste porosity (helium)	0·113	0·311	0·202
	Concrete porosity (helium)	0·583	0·391	0·162
	Paste porosity (mercury)	0·409	0·376	0·135
	Calculated paste porosity		0·419	
	Calculated concrete porosity		0·402	
Inverse of cube strength N/mm^2	Paste porosity (helium)	0·671	0·861	0·602
	Concrete porosity (helium)	0·450	0·901	0·157
	Paste porosity (mercury)	0·780	0·941	0·683
	Calculated paste porosity		0·944	
	Calculated concrete porosity		0·884	
Log of initial resistance ohms	Paste porosity (helium)	0·208	0·741	0·294
	Concrete porosity (helium)	0·232	0·726	0·228
	Paste porosity (mercury)	0·279	0·769	0·301
	Calculated paste porosity		0·813	
	Calculated concrete porosity		0·613	
Log of 28 day resistance ohms	Paste porosity (helium)	0·276	0·701	0·808
	Concrete porosity (helium)	0·589	0·763	0·669
	Paste porosity (mercury)	0·532	0·801	0·753
	Calculated paste porosity		0·850	
	Calculated concrete porosity		0·632	

Pore size ranges in mercury intrusion. For the main transport properties attempts were made to develop multiple regression models based on the porosities from different pore size ranges obtained from mercury intrusion. It was hoped that the different characteristics of the pore size distributions would combine in linear combinations to form a predictive model. It was found, however, that in each case a single predictor model based on the total porosity could not be improved by including any of the individual pore size ranges. This might be expected from the negative correlation between total porosity and some of the porosities in size ranges.

Chloride transport. The relationship between chloride concentration and paste porosity measured by mercury intrusion is shown in Fig. 8. The measured chloride concentration will be proportional to the chloride transport to the point of measurement. It may be seen that the porosity measurement woks as an excellent predictor and the correlation coefficient is 0·77. If the porosity from helium intrusion is used (Fig. 9) it may be seen that the transport would be over

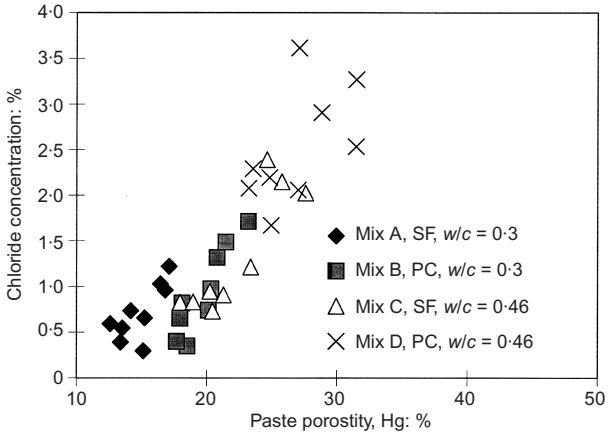

Fig. 8. Chloride concentration from diffusion test vs. mercury intrusion porosity

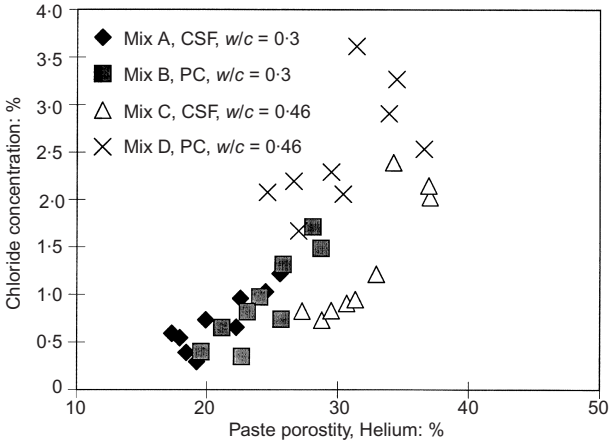

Fig. 9. Chloride concentration from diffusion test vs. helium intrusion porosity

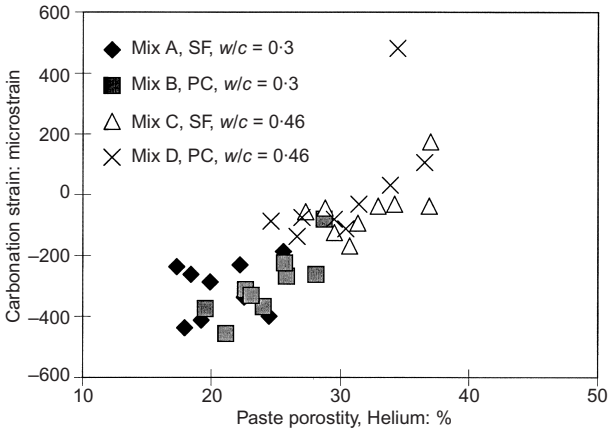

Fig. 10. Carbonation strain vs. helium intrusion porosity

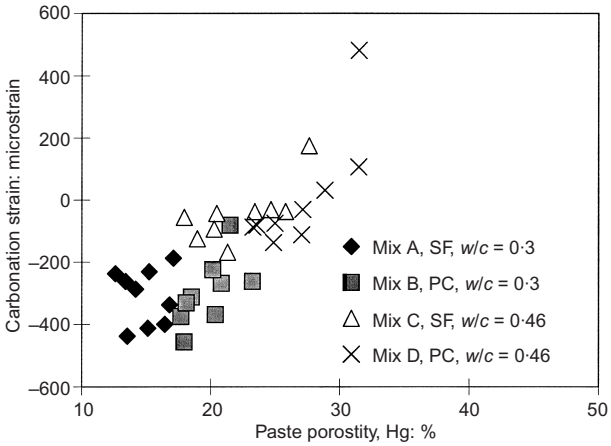

Fig. 11. Carbonation strain vs. mercury intrusion porosity

estimated for mix C, which is the SF mix with the higher w/c ratio. Looking at the relationship between the mercury and helium porosities (Fig. 2) it may be seen that mix C has a higher than expected porosity from the helium intrusion. It is concluded from these observations that mix C has a substantial closed porosity which was not accessed by the mercury because the samples were not ground before the mercury test and because the higher viscosity of the mercury. This closed porosity would not contribute to the chloride transport.

For the PC samples alone all three different methods of measuring porosity gave high correlations of porosity with chloride concentration in the range 0·65–0·08.

Carbonation. The relationships between carbonation strain and helium and mercury porosity are similar (Figs 10 and 11). The Helium porosity shows a slightly higher correlation (see Table 6) but both measurements may be taken as equally good predictors of carbonation.

Oxygen transport. The observed values of oxygen permeability had a range of several orders of magnitude and none of the measured porosities were good predictors for them. It was found, however, that the log of the oxygen permeability could be predicted with porosity. For the PC samples all of the measurements of porosity gave R^2 in the range 0·7–0·8. For the SF the correlations are far lower and the reason for this may be seen from Fig. 12 which shows the relationship with the porosity from mercury intrusion. It may be seen that there are some SF samples which had low porosity but high permeability giving an apparent decrease in permeability with increasing porosity for the lower porosity samples of mixes A and C. This might have been caused by the creation of a connected pore system when the calcium hydroxide is depleted by the pozzolanic reaction, but there is no other evidence to support this explanation and microcracking of the higher strength samples during drying is probably more likely.

Water vapour transport. It has been shown[9] that, in the experiments that were carried out, the water vapour transport rate was controlled by the rate of evaporation

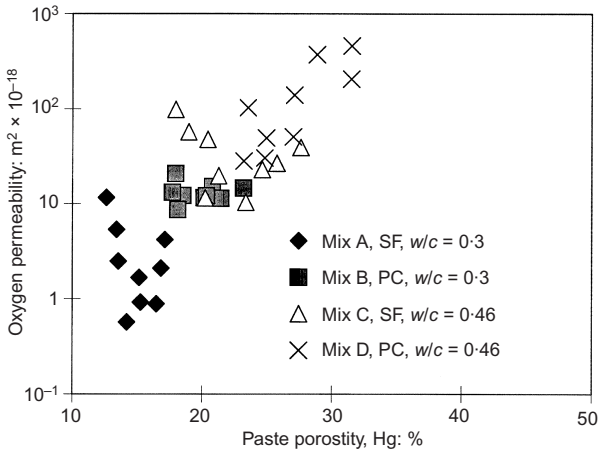

Fig. 12. Oxygen permeability vs. mercury intrusion porosity

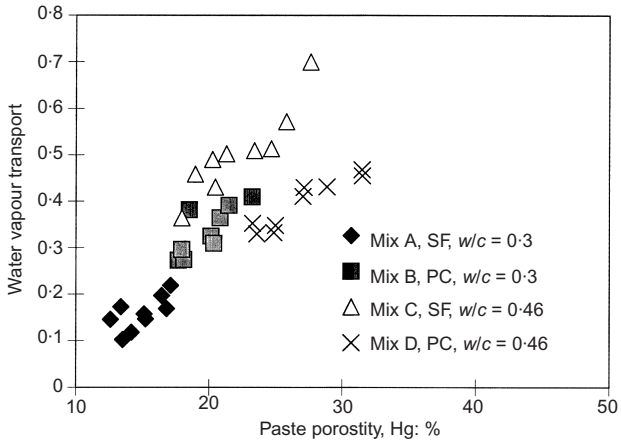

Fig. 14. Water vapour transport (relative units) vs. mercury intrusion porosity

from the low humidity side of the sample. This rate of evaporation rate will depend on the surface area of the pores exposed on the surface and this area will, in turn, depend on the total porosity. It may be seen that, as expected from this, the correlation is highest with the helium intrusion. Looking at the relationships in Figs 13 and 14 it is apparent that mix D is the cause of the poorer relationship with mercury intrusion results. This will be because all of the other mixes have a higher proportion of closed porosity.

Corrosion currents. The models for corrosion currents were poorer than those for the transport properties indicating that there may not be a causal link between porosity and corrosion other than the indirect one through the transport properties. The log of the corrosion current was used because this gave the best models. The initial corrosion measurement was made directly after the samples were placed in the saline solution. The 28 day measurement was made after 28 days of corrosion driven by a 100 mV anodic voltage. This voltage will have caused migration of the chloride ions so the resultant corrosion rates would be expected to correlate more with porosity (through the transport properties) than the initial corrosion rates. The correlations are, however, all low and it may be seen from the relationship between the 28 day corrosion and the concrete porosity from helium intrusion (Fig. 15) which has the highest correlation that they largely depend on the mix D samples having generally high porosity and high corrosion.

Cube strength. In order to obtain a good predictive model the inverse of the cube strength was used. The relationship with the calculated paste porosity was excellent (for PC samples only). In this case the strength is likely to be used as the predictor for porosity, the relationship with mercury porosity may be seen in Fig. 16.

Resistivity. In order to obtain better predictions the log of the resistance values was used in all cases. The relationship between porosity and initial resistance is clearest in Fig. 17. giving the results from helium

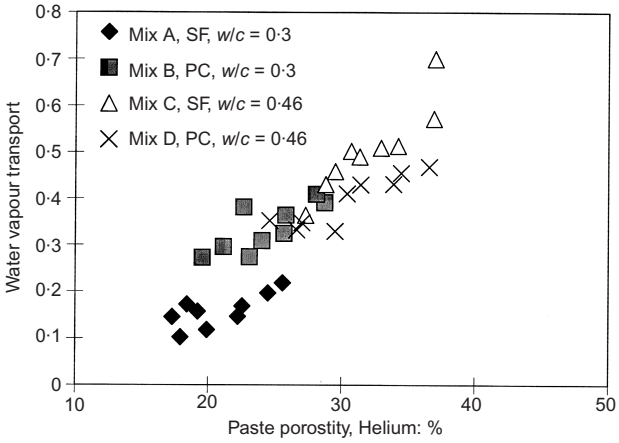

Fig. 13. Water vapour transport (relative units) vs. helium intrusion porosity

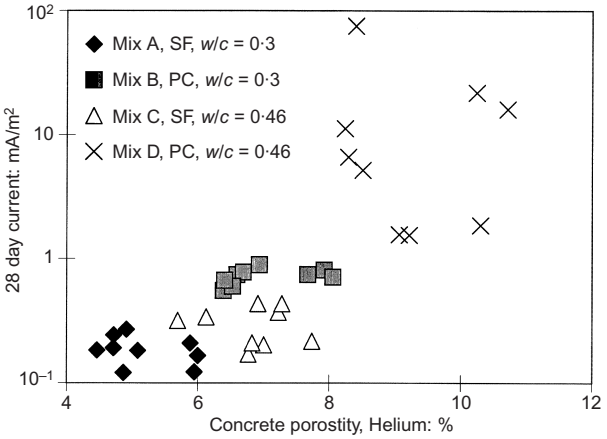

Fig. 15. Corrosion current at 28 days of test vs. helium intrusion porosity

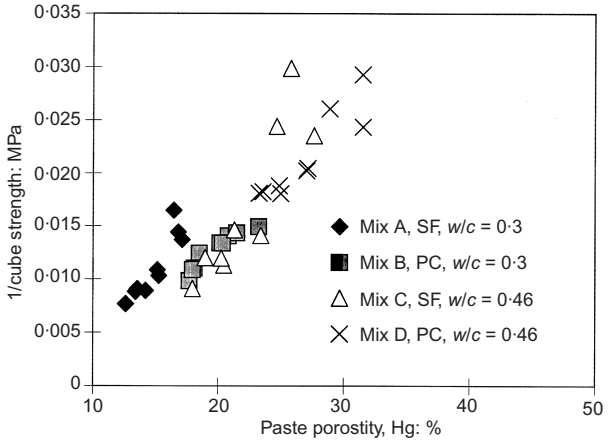

Fig. 16. Inverse of cube strength vs. mercury intrusion porosity

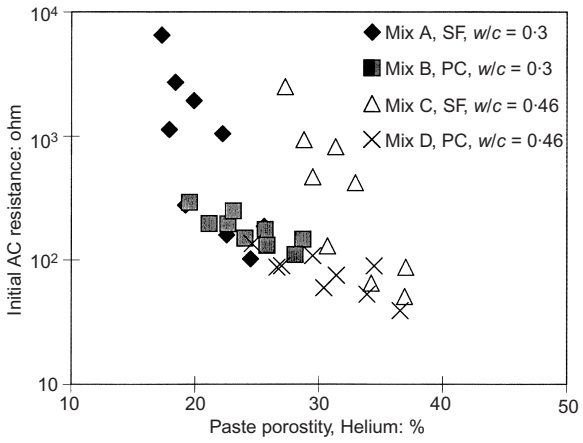

Fig. 17. Electrical resistance at start of corrosion test vs. helium intrusion porosity

intrusion. The PC results and the SF results from tests at age 3 days all like on a clear line, the 28 day results from cold curing (CC3) also lie on this line. The other SF samples lie above the line. This increase in resistance has been caused by the depletion of lime by the pozzolanic reaction and is independent of porosity.[14] After 28 days of anodic polarisation all of the SF samples have high resistivity due to lime depletion and lie on a separate clear line (Fig. 18). Because all of the resistance samples were the same size the resistivity values for the materials will be proportional to the measured resistances.

Conclusions

(*a*) The results of this article indicate that when using measurements of porosity as predictors for bulk concrete properties it is equally valid to use measurements on paste or concrete samples.

(*b*) In this article models using total porosity to predict the performance of the concrete could not be improved by including data for the individual pore size ranges from mercury intrusion.

(*c*) Mercury intrusion is the best predictor of chloride transport because the mercury does not penetrate closed porosity and this closed porosity does not contribute to the transport.

(*d*) Helium intrusion is the best predictor of water vapour transport if it is controlled by evaporation because it will depend on the total porosity.

(*e*) Corrosion rates are not predicted as well as transport properties by models based on porosity.

(*f*) The resistivity of concrete is predicted well by porosity models but for mixes containing SF the effect of lime depletion by the pozzolanic reaction has a more significant effect.

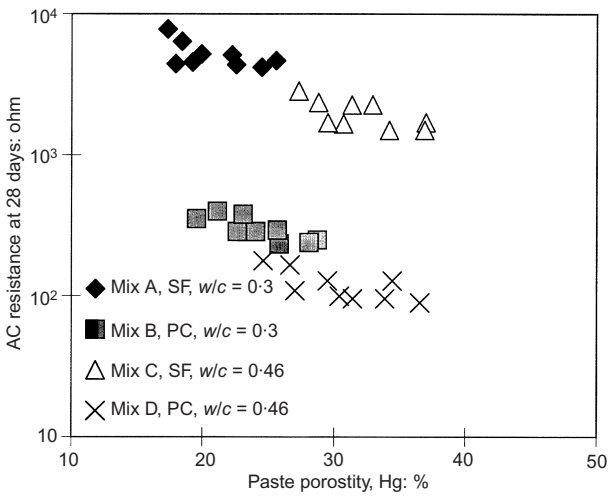

Fig. 18. Electrical resistance after 28 days of test vs. mercury intrusion porosity

References

1. NEVILLE A. M. *Properties of concrete*, 4th edn., Longman, London, 1995.
2. ACI Committee 226. Silica fume in concrete—a report, *ACI Materials Journal*, March–April.
3. FELDMAN R. F. and CHENG Yi. H. Properties of Portland cement – silica fume pastes 1. Porosity and surface properties, *Cement and Concrete Research*, 1985, **15**, 765–774.
4. CABRERA J. G., CLAISSE P. A. and HUNT D. N. A statistical analysis of the factors which contribute to the corrosion of steel in OPC and Silica Fume Concrete, *Construction and Building Materials*, 1995, **9**, No. 1, 105–113.
5. KUMAR A., KOMARNENI S. and ROY D. M. Diffusion of Cs^+ and Cs^- through Sealing Materials, *Cement and Concrete Research*, 1987, **17**, 153–160.
6. TENOUTASSE N. and MARION A. M. Drying shrinkage and creep of concrete with condensed silica fume, *ACI Special Publication SP91*, Supplementary vol. 3, 1986.
7. BUIL M. and DELAGE P. Some further evidence on a specific effect of silica fume on the pore structure of Portland cement mortars, *Cement and Concrete Research*, 1987, **17**, 65–69.
8. CABRERA J. G. and CLAISSE P. A. Measurement of chloride

penetration into silica fume concrete, *Cement and Concrete Composites*, 1990, **12**, 157–161.
9. CABRERA J. G. and CLAISSE P. A. Oxygen and water transport in cement-silica fume pastes. *Construction and Building Materials*, 1999, **13**, 405–414.
10. CLAISSE P. A. The properties and performance of high strength silica fume concrete. PhD thesis, University of Leeds, 1988.
11. CABRERA J. G. and CLAISSE P. A. Corrosion measurements on reinforcement in silica fume concrete. *Arabian Journal for Science and Engineering*, 1995, **20**, No. 2, 259–267.
12. CABRERA J. G., CLAISSE P. A. and LYNSDALE C. J. Application of microcomputers in the retrieval and processing of data in the study of the durability of reinforced concrete. *Materials and Structures*, 1993, **26**, 587–593.
13. CABRERA J. G. The porosity of concrete. Concrete research seminar, Leeds 1985.
14. CABRERA J. G. and CLAISSE P. A. The effect of curing conditions on the properties of silica fume concrete, in *Blended Cements in Construction* (Swamy R. N. (Ed.), *Proc. Int. Conf. Sheffield*, 9–12 September, 1991, Elsevier, London.

Discussion contributions on this paper should reach the editor by 31 January 2002